

Exclusive production of ϕ meson in the $\gamma^* p \rightarrow \phi p$ reaction at large photon virtualities within k_T -factorization approach

A.D. Bolognino^{1,2,*}, A. Szczurek^{3,4,§}, W. Schäfer^{4,‡}

¹ *Dipartimento di Fisica, Università della Calabria
I-87036 Arcavacata di Rende, Cosenza, Italy*

² *Istituto Nazionale di Fisica Nucleare, Gruppo collegato di Cosenza
I-87036 Arcavacata di Rende, Cosenza, Italy*

³ *College of Natural Sciences, Institute of Physics, University of Rzeszów
ul. Pigonia 1, PL-35-310 Rzeszów, Poland*

⁴ *Institute of Nuclear Physics Polish Academy of Sciences
ul. Radzikowskiego 152, PL-32-342, Kraków, Poland*

Abstract

We apply the k_T -factorization approach to the production of ϕ meson in deep-inelastic scattering. The helicity-conserving $\gamma^*(T, L) \rightarrow \phi$ impact factor is calculated for longitudinal and transverse photon polarization using ϕ meson distribution amplitudes. Different unintegrated gluon distributions are used in the calculations. The formalism for massless quarks/antiquarks gives too large transverse and longitudinal cross sections for photon virtualities below $Q^2 \sim 8 \text{ GeV}^2$. We suggest how to improve the description of the HERA data by introducing effective strange quark masses into the formalism. We derive the corresponding massive impact factor by comparing to the light-cone wave function representation used in previous k_T -factorization calculations and the color-dipole approaches. As a byproduct we present expressions for higher twist-amplitudes as weighted integrals over the light-cone wave function. The quark mass $m_q \approx 0.5 \text{ GeV}$ allows to improve the description of both longitudinal and transverse cross section down to $Q^2 \sim 4 \text{ GeV}^2$. We present also the polarized cross section ratio σ_L/σ_T and the behavior of the total cross section $\sigma_{tot} = \sigma_L + \sigma_T$ as a function of photon virtuality.

**e-mail:* ad.bolognino@unical.it

§*e-mail:* antoni.szczurek@ifj.edu.pl

‡*e-mail:* wolfgang.schafer@ifj.edu.pl

1 Introduction

The diffractive electroproduction of vector mesons, $\gamma^* p \rightarrow Vp$, has attracted much attention at the HERA collider (for a review see e.g. Ref. [1]) and is to be expected an important subject in future experiments e.g. at an electron-ion collider (EIC) [2]. In this work we are interested in the limit of large $\gamma^* p$ center-of-mass energy W , $s \equiv W^2 \gg Q^2 \gg \Lambda_{\text{QCD}}^2$, which implies small gluon longitudinal fraction $x = (Q^2 + m_V^2)/(W^2 + Q^2 - m_p^2) \sim Q^2/W^2$. In this kinematics, the photon virtuality Q^2 gives a handle on the dominant size of color dipoles in the $\gamma^* \rightarrow V$ transition and thus allows to study a transition from the hard, perturbative (small dipole), to the soft, nonperturbative (large dipole), regimes of scattering. In momentum space, the color dipole approach has its correspondence in the k_T -factorization, where the main ingredient is the unintegrated (transverse-momentum dependent) gluon distribution (UGD). At large photon virtualities the diffractive cross section is a sensitive probe of the proton UGD.

The k_T -factorization formalism reviewed in Ref. [1], includes besides the transverse momentum of gluons also the transverse momentum of quark and antiquark in the vector meson as encoded in the light-cone wave function of the meson. This approach was used with some success in Ref. [3]. At very large Q^2 one may expect, that the relative transverse motion of (anti-)quarks in the bound state becomes negligible, and can be integrated out. Then, regarding the vector meson only a dependence on the longitudinal momentum fraction of quarks encoded in distribution amplitudes (DA) is left.

A quite general factorization formalism of vector meson production in deep inelastic scattering was formulated in Refs. [4, 5] and has been recently applied in Ref. [6] to the diffractive deep inelastic production of ρ mesons. While the production of longitudinal vector mesons involves the leading twist DA, similar to the one introduced for other hadronic processes in Refs. [7, 8, 9, 10], for transverse vector mesons higher twists are involved and corresponding DAs studied in Ref. [11] are needed.

The recent analysis of helicity amplitudes for ρ^0 meson production [6] showed that this approach may be useful in testing UGDs. In this paper, in order to test the formalism further, we wish to focus on and investigate the exclusive photoproduction of ϕ meson:

$$\gamma^* p \rightarrow \phi p .$$

Corresponding experimental data were obtained by the H1 [12, 13] and ZEUS [14] collaborations at HERA. In this paper we will show how the k_T -factorization approach of [15] matches to the higher-twist DA expansion, at least in the Wandzura-Wilczek (WW) approximation, where no explicit $q\bar{q}g$ contributions are included. Future applications at EIC may require the inclusion of next-to-leading-order contributions.

Here the approach based on DAs has the advantage that for the case of collinear partons in the final state, the necessary techniques for the calculation of NLO impact factors are well advanced [16, 17]. The first part of the paper is devoted to the summary of the theoretical framework of calculating the helicity amplitudes within the k_T -factorization approach. The second part shows the cross sections of the process and the effects due to UGDs and/or due to the strange-quark mass. Here we take advantage of the fact that we can rather straightforwardly derive the massive impact factor in the WW approximation from the light-cone wave function approach. As a byproduct we show how higher twist DAs can be obtained from the light-cone wave functions which may be interesting for the application of various light-cone models also to other vector mesons.

A comparison with the H1 and ZEUS measurements will be presented. The conclusion section will close our paper.

2 Theoretical framework

2.1 Helicity-amplitudes $T_{\lambda_V \lambda_\gamma}$

In the high-energy regime, $s \equiv W^2 \gg Q^2 \gg \Lambda_{\text{QCD}}^2$, which implies small $x = (Q^2 + m_V^2)/(W^2 + Q^2 - m_p^2) \sim Q^2/W^2$, the forward helicity amplitude $T_{\lambda_V \lambda_\gamma}$ can be expressed, in the k_T -factorization, as the convolution of the $\gamma^* \rightarrow V$ impact factor (IF), $\Phi_{\lambda_V, \lambda_\gamma}^{\gamma^* \rightarrow V}(\kappa^2, Q^2)$, with the UGD, $\mathcal{F}(x, \kappa^2)$.

Our normalization of the impact factor is chosen, such that the forward amplitude for the $\gamma^* p \rightarrow V p$ process reads

$$\Im m T_{\lambda_V \lambda_\gamma}(s, Q^2) = s \int \frac{d^2 \kappa}{(\kappa^2)^2} \Phi_{\lambda_V, \lambda_\gamma}^{\gamma^* \rightarrow V}(\kappa^2, Q^2) \mathcal{F}(x, \kappa^2). \quad (1)$$

Here, the UGD is related to the collinear gluon parton distribution as

$$xg(x, \mu^2) = \int^{\mu^2} \frac{d\kappa^2}{\kappa^2} \mathcal{F}(x, \kappa^2). \quad (2)$$

We now turn to the two different approaches to the impact factors which we want to compare in this work.

2.2 Distribution amplitude expansion

We start with the scheme based on the collinear factorization of the meson structure which was worked out in Refs. [4, 5] and was used recently for ρ -meson electroproduction in Ref. [6]. This approach starts from the observation, that at large Q^2 the transverse internal motion of partons in the meson can be neglected.

The longitudinal impact factor is expressed in terms of the standard twist-2 distribution amplitude. In the normalization adopted by us, the IF for the $L \rightarrow L$

transition reads

$$\Phi_{0,0}^{\gamma^* \rightarrow V}(\boldsymbol{\kappa}^2, Q^2) = \frac{4\pi\alpha_S e_q \sqrt{4\pi\alpha_{\text{em}}} f_V}{N_c Q} \int_0^1 dy \varphi_1(y; \mu^2) \left(\frac{\alpha}{\alpha + y\bar{y}} \right), \quad (3)$$

where $\alpha = \boldsymbol{\kappa}^2/Q^2$, y is the fraction of the mesons's lightcone-plus momentum carried by the quark, $\bar{y} = 1 - y$, and $\varphi_1(y; \mu^2)$ is the twist-2 distribution amplitude (DA). It is normalized as

$$\int_0^1 dy \varphi_1(y; \mu^2) = 1 \quad (4)$$

and we recall its asymptotic form

$$\varphi_1(y; \mu^2) \xrightarrow{\mu^2 \rightarrow \infty} \varphi_1^{as}(y) = 6y\bar{y}. \quad (5)$$

The expression for the transverse case is:

$$\begin{aligned} \Phi_{+,+}^{\gamma^* \rightarrow V}(\boldsymbol{\kappa}^2, Q^2) &= \frac{2\pi\alpha_S e_q \sqrt{4\pi\alpha_{\text{em}}} f_V m_V}{N_c Q^2} \\ &\times \left\{ \int_0^1 dy \frac{\alpha(\alpha + 2y\bar{y})}{y\bar{y}(\alpha + y\bar{y})^2} \left[(y - \bar{y})\varphi_1^T(y; \mu^2) + \varphi_A^T(y; \mu^2) \right] \right. \\ &- \int_0^1 dy_2 \int_0^{y_2} dy_1 \frac{y_1 \bar{y}_1 \alpha}{\alpha + y_1 \bar{y}_1} \\ &\times \left[\frac{2 - N_c/C_F}{\alpha(y_1 + \bar{y}_2) + y_1 \bar{y}_2} - \frac{N_c/C_F}{y_2 \alpha + y_1(y_2 - y_1)} \right] M(y_1, y_2; \mu^2) \\ &+ \int_0^1 dy_2 \int_0^{y_2} dy_1 \left[\frac{2 + N_c/C_F}{\bar{y}_1} + \frac{y_1}{\alpha + y_1 \bar{y}_1} \left(\frac{(2 - N_c/C_F)y_1 \alpha}{\alpha(y_1 + \bar{y}_2) + y_1 \bar{y}_2} - 2 \right) \right. \\ &\left. \left. - \frac{N_c}{C_F} \frac{(y_2 - y_1)\bar{y}_2}{\bar{y}_1} \frac{1}{\alpha \bar{y}_1 + (y_2 - y_1)\bar{y}_2} \right] S(y_1, y_2; \mu^2) \right\}, \quad (6) \end{aligned}$$

where:

$$C_F = \frac{N_c^2 - 1}{2N_c}, \quad (7)$$

$$B(y_1, y_2; \mu^2) = -5040 y_1 \bar{y}_2 (y_1 - \bar{y}_2)(y_2 - y_1), \quad (8)$$

$$D(y_1, y_2; \mu^2) = -360 y_1 \bar{y}_2 (y_2 - y_1) \left(1 + \frac{\omega_{\{1,0\}}^A(\mu^2)}{2} (7(y_2 - y_1) - 3) \right), \quad (9)$$

and where the three-body DAs read:

$$M(y_1, y_2; \mu^2) = \zeta_{3V}^V(\mu^2) B(y_1, y_2; \mu^2) - \zeta_{3V}^A(\mu^2) D(y_1, y_2; \mu^2), \quad (10)$$

$$S(y_1, y_2; \mu^2) = \zeta_{3V}^V(\mu^2) B(y_1, y_2; \mu^2) + \zeta_{3V}^A(\mu^2) D(y_1, y_2; \mu^2) \quad (11)$$

with the dimensionless coupling constants $\zeta_{3V}^V(\mu^2)$ and $\zeta_{3V}^A(\mu^2)$ defined as

$$\zeta_{3V}^V(\mu^2) = \frac{f_{3V}^V(\mu^2)}{f_V}, \quad \zeta_{3V}^A(\mu^2) = \frac{f_{3V}^A(\mu^2)}{f_V}. \quad (12)$$

The dependence on the factorization scale μ^2 can be determined from evolution equations [11] (see also Appendix B in Ref. [5]), with the initial condition at a renormalization scale $\mu_0 = 1$ GeV.

The DAs $\varphi_1^T(y; \mu^2)$ and $\varphi_A^T(y; \mu^2)$ in Eq. (6) encompass both genuine twist-3 and Wandzura-Wilczek (WW) contributions¹ [11].

2.3 Light-cone wave function (LCWF) approach

In the light-cone k_T -factorization approach, the calculation proceeds in a slightly different way. Here one calculates the amplitude for the $\gamma^* p \rightarrow q\bar{q}p$ diffractive process and projects the final state $q\bar{q}$ pair onto the vector meson state. We treat the ϕ -meson as a pure $s\bar{s}$ state. The meson of momentum $P = (P_+, m_\phi^2/(2P_+), \mathbf{0})$ is described by the $s\bar{s}$ light cone wave function as

$$|\phi, P_+, \lambda_V\rangle = \int \frac{dy d^2\mathbf{k}}{y\bar{y}} \Psi_{\lambda\bar{\lambda}}^{(\lambda_V)}(y, \mathbf{k}) |s(yP_+, \mathbf{k}, \lambda) \bar{s}(\bar{y}P_+, -\mathbf{k}, \bar{\lambda})\rangle + \dots \quad (13)$$

The amplitude for diffractive vector meson production then takes the form

$$\Im m T_{\lambda_V, \lambda_\gamma}(s, Q^2) = s \int \frac{dy d^2\mathbf{k}}{y\bar{y} 16\pi^3} \sum_{\lambda\bar{\lambda}} \mathcal{M}_{\lambda\bar{\lambda}}^{(\lambda_\gamma)}(\gamma^* p \rightarrow s\bar{s}p) \Psi_{\lambda\bar{\lambda}}^{(\lambda_V)*}(y, \mathbf{k}). \quad (14)$$

The explicit expressions for the diffractive amplitudes can be found in Ref. [1]. Here we are interested only in the forward scattering limit of vanishing transverse momentum transfer, where only the helicity conserving amplitudes with $\lambda_V = \lambda_\gamma$ contribute.

We can easily read off the following expressions for the impact factors of interest. The $L \rightarrow L$ IF reads

$$\begin{aligned} \Phi_{0,0}^{\gamma^* \rightarrow \phi}(\boldsymbol{\kappa}^2, Q^2) &= \sqrt{4\pi\alpha_{\text{em}}} e_q 8\pi\alpha_S(\mu^2) Q \int \frac{dy d^2\mathbf{k}}{\sqrt{y\bar{y}} 16\pi^3} I_0(\mathbf{k}, \boldsymbol{\kappa}) \\ &\times y\bar{y} \left\{ \Psi_{+-}^{(0)*}(y, \mathbf{k}) + \Psi_{-+}^{(0)*}(y, \mathbf{k}) \right\}. \end{aligned} \quad (15)$$

For the $T \rightarrow T$ IF we obtain

$$\begin{aligned} \Phi_{\pm, \pm}^{\gamma^* \rightarrow \phi}(\boldsymbol{\kappa}^2, Q^2) &= \sqrt{4\pi\alpha_{\text{em}}} e_q 4\pi\alpha_S(\mu^2) \int \frac{dy d^2\mathbf{k}}{\sqrt{y\bar{y}} 16\pi^3} \\ &\times \left[(e(\pm) \cdot \mathbf{I}_1(\mathbf{k}, \boldsymbol{\kappa})) \left\{ (y - \bar{y}) \left(\Psi_{+-}^{(\pm)*}(y, \mathbf{k}) + \Psi_{-+}^{(\pm)*}(y, \mathbf{k}) \right) \right. \right. \\ &\quad \left. \left. + \Psi_{+-}^{(\pm)*}(y, \mathbf{k}) - \Psi_{-+}^{(\pm)*}(y, \mathbf{k}) \right\} + \sqrt{2} m_q I_0(\mathbf{k}, \boldsymbol{\kappa}) \Psi_{++}^{(\pm)*}(y, \mathbf{k}) \right]. \end{aligned} \quad (16)$$

¹Genuine terms are related to $B(y_1, y_2; \mu^2)$ and $D(y_1, y_2; \mu^2)$; WW contributions, instead, are those obtained in the approximation in which $B(y_1, y_2; \mu^2) = D(y_1, y_2; \mu^2) = 0$. For their expressions in this last case see Eq. (9) in Refs. [5, 6].

Here

$$I_0(\mathbf{k}, \boldsymbol{\kappa}) = \frac{1}{\mathbf{k}^2 + \varepsilon^2} - \frac{1}{(\mathbf{k} + \boldsymbol{\kappa})^2 + \varepsilon^2}, \quad I_1(\mathbf{k}, \boldsymbol{\kappa}) = \frac{\mathbf{k}}{\mathbf{k}^2 + \varepsilon^2} - \frac{\mathbf{k} + \boldsymbol{\kappa}}{(\mathbf{k} + \boldsymbol{\kappa})^2 + \varepsilon^2}, \quad (17)$$

and $\varepsilon^2 = m_q^2 + y\bar{y}Q^2$. We now want to compare these results with the twist expansion approach presented in the previous chapters. To this end, we should expand the impact factors around the limit of collinear kinematics for the $q\bar{q}$ -pair. While an analogous expansion around the small- $\boldsymbol{\kappa}$ limit, has been discussed in great detail, the analogous comparison to leading and higher twist distribution amplitudes is up to now missing.

Expanding in $\mathbf{k}^2/(\boldsymbol{\kappa}^2 + \varepsilon^2) \ll 1$, we obtain

$$I_0(\mathbf{k}, \boldsymbol{\kappa}) \approx \frac{1}{\varepsilon^2} - \frac{1}{\boldsymbol{\kappa}^2 + \varepsilon^2} = \frac{\boldsymbol{\kappa}^2}{\varepsilon^2(\boldsymbol{\kappa}^2 + \varepsilon^2)}, \quad (18)$$

and

$$I_1(\mathbf{k}, \boldsymbol{\kappa}) \approx \mathbf{k} \frac{\boldsymbol{\kappa}^2}{\varepsilon^2(\boldsymbol{\kappa}^2 + \varepsilon^2)} + \frac{2(\mathbf{k} \cdot \boldsymbol{\kappa})\boldsymbol{\kappa}}{(\boldsymbol{\kappa}^2 + \varepsilon^2)^2} \rightarrow \frac{\boldsymbol{\kappa}^2(\boldsymbol{\kappa}^2 + 2\varepsilon^2)}{\varepsilon^2(\boldsymbol{\kappa}^2 + \varepsilon^2)^2} \mathbf{k}, \quad (19)$$

where we performed the azimuthal average in the last step. Inserting the expanded I_0 into the LL IF, we find

$$\begin{aligned} \Phi_{0,0}^{\gamma^* \rightarrow \phi}(\boldsymbol{\kappa}^2, Q^2) &= \sqrt{4\pi\alpha_{\text{em}}}e_q 8\pi\alpha_S(\mu^2)Q \int_0^1 dy y\bar{y} \frac{\boldsymbol{\kappa}^2}{\varepsilon^2(\boldsymbol{\kappa}^2 + \varepsilon^2)} \\ &\times \frac{1}{\sqrt{y\bar{y}}} \int \frac{d^2\mathbf{k}}{16\pi^3} \left\{ \Psi_{+-}^{(0)*}(y, \mathbf{k}) + \Psi_{-+}^{(0)*}(y, \mathbf{k}) \right\} \theta(\mu^2 - \mathbf{k}^2) \\ &= \sqrt{4\pi\alpha_{\text{em}}}e_q \frac{4\pi\alpha_S(\mu^2)f_V}{N_c Q} \int_0^1 dy \frac{y\bar{y}}{(y\bar{y} + \tau)} \frac{\alpha}{(\alpha + y\bar{y} + \tau)} \varphi_1(y, \mu^2). \end{aligned} \quad (20)$$

Here we introduced the variables $\alpha = \boldsymbol{\kappa}^2/Q^2$ and $\tau = m_q^2/Q^2$. We see that we have obtained a generalization to finite quark mass of the impact factor of Eq. (3). The helicity combination of the LCWF which appears under the \mathbf{k} integral gives rise to the leading twist distribution amplitude of the longitudinally polarized vector meson, defined following the rules of Ref. [9] as

$$f_V \varphi_1(y, \mu_0^2) = \frac{2N_c}{\sqrt{y\bar{y}}} \int \frac{d^2\mathbf{k}}{16\pi^3} \theta(\mu_0^2 - \mathbf{k}^2) \left\{ \Psi_{+-}^{(0)*}(y, \mathbf{k}) + \Psi_{-+}^{(0)*}(y, \mathbf{k}) \right\}. \quad (21)$$

The scale μ^2 in Eq. (20) must be chosen such that the small- \mathbf{k} expansion is valid, i.e. $\mu^2 \sim (Q^2 + m_\phi^2)/4$.

We can now follow a similar strategy for the transverse IF. To that end we introduce the following representations of the higher twist DA's:

$$\begin{aligned} f_V \varphi_1^T(y, \mu_0^2) &= \frac{2N_c}{\sqrt{y\bar{y}}} \int \frac{d^2\mathbf{k}}{16\pi^3} \theta(\mu_0^2 - \mathbf{k}^2) (e(\pm) \cdot \mathbf{k}) \left\{ \Psi_{+-}^{(\pm)*}(y, \mathbf{k}) + \Psi_{-+}^{(\pm)*}(y, \mathbf{k}) \right\}, \\ f_V \varphi_A^T(y, \mu_0^2) &= \frac{2N_c}{\sqrt{y\bar{y}}} \int \frac{d^2\mathbf{k}}{16\pi^3} \theta(\mu_0^2 - \mathbf{k}^2) (e(\pm) \cdot \mathbf{k}) \left\{ \Psi_{+-}^{(\pm)*}(y, \mathbf{k}) - \Psi_{-+}^{(\pm)*}(y, \mathbf{k}) \right\}, \\ f_V \varphi_m(y, \mu_0^2) &= \frac{2N_c}{\sqrt{y\bar{y}}} \int \frac{d^2\mathbf{k}}{16\pi^3} \theta(\mu_0^2 - \mathbf{k}^2) \sqrt{2}m_q \Psi_{++}^{(\pm)*}(z, \mathbf{k}). \end{aligned} \quad (22)$$

We notice, that

$$\int_0^1 dy \varphi(y, \mu_0^2) = 1, \quad \int_0^1 dy \varphi_1^T(y, \mu_0^2) = 0. \quad (23)$$

The transverse IF that we derive is again a massive generalization of Eq. (6) and reads

$$\begin{aligned} \Phi_{\pm, \pm}^{\gamma \rightarrow \phi}(\kappa^2, Q^2) &= \sqrt{4\pi\alpha_{\text{em}}e_q} \frac{2\pi\alpha_S(\mu^2)f_V}{N_c Q^2} \int_0^1 \frac{dy}{y\bar{y} + \tau} \left\{ \frac{\alpha(\alpha + 2y\bar{y} + 2\tau)}{(\alpha + y\bar{y} + \tau)^2} \right. \\ &\quad \times \left((y - \bar{y})\varphi_1^T(y, \mu^2) + \varphi_1^A(y, \mu^2) \right) + \frac{\alpha}{\alpha + y\bar{y} + \tau} \varphi_m(y, \mu^2) \left. \right\}. \end{aligned} \quad (24)$$

We realize that up to the DA φ_m , which vanishes in the massless limit, the structure of the IF is exactly the same as for the one of Eq. (6) neglecting the so-called genuine three particle distributions. The latter obviously can appear only at the level of the $q\bar{q}g$ -Fock state.

We now wish to give some explicit expressions for the DA's in question. To this end, we use the $V \rightarrow q\bar{q}$ vertex from Ref. [1], where the ϕ -meson is treated as a pure S -wave bound state of strange quark and antiquark. For the relevant combinations of light-cone wave functions we obtain in the case of the longitudinally polarized vector meson:

$$\Psi_{+-}^{(0)*}(y, \mathbf{k}) + \Psi_{-+}^{(0)*}(y, \mathbf{k}) = -4M\sqrt{y\bar{y}} \left\{ 1 + \frac{(y - \bar{y})^2}{4y\bar{y}} \frac{2m_q}{M + 2m_q} \right\} \psi(y, \mathbf{k}). \quad (25)$$

The radial wave function $\psi(z, \mathbf{k})$ is normalized as

$$N_c \int \frac{dz d^2\mathbf{k}}{y\bar{y} 16\pi^3} 2M^2 |\psi(y, \mathbf{k})|^2 = 1. \quad (26)$$

Above $M^2 = (\mathbf{k}^2 + m_q^2)/(y\bar{y})$ is the invariant mass of the $s\bar{s}$ -system. We can now express the leading twist DA through the radial WF as

$$f_V \varphi_1(y, \mu_0^2) = \frac{N_c}{2\pi^2} \int_0^{\mu_0^2} d\mathbf{k}^2 M \left\{ 1 + \frac{(y - \bar{y})^2}{4y\bar{y}} \frac{2m_q}{M + 2m_q} \right\} \psi(y, \mathbf{k}). \quad (27)$$

Now, for the higher twist DA's of the transversely polarized vector meson, we obtain

$$\begin{aligned} f_V \varphi_1^T(y, \mu_0^2) &= (y - \bar{y}) \frac{N_c}{8\pi^2} \int_0^{\mu_0^2} d\mathbf{k}^2 \mathbf{k}^2 \frac{M}{M + 2m_q} \frac{\psi(y, \mathbf{k})}{y\bar{y}}, \\ f_V \varphi_A^T(y, \mu_0^2) &= \frac{N_c}{4\pi^2} \int_0^{\mu_0^2} d\mathbf{k}^2 \mathbf{k}^2 \frac{\psi(y, \mathbf{k})}{y\bar{y}}, \\ f_V \varphi_m(y, \mu_0^2) &= m_q^2 \frac{N_c}{4\pi^2} \int_0^{\mu_0^2} d\mathbf{k}^2 \left\{ 1 + \frac{\mathbf{k}^2}{m_q(M + 2m_q)} \right\} \frac{\psi(y, \mathbf{k})}{y\bar{y}}. \end{aligned} \quad (28)$$

2.4 Characteristic parameters

Typical constants for ϕ meson, entering DAs and IFs, used in numerical computations, are provided in the following tables:

V	ϕ
$f_V[\text{GeV}]$	0.254
ζ_{3V}^A	0.032
ζ_{3V}^V	0.013
$\omega_{1,0}^A$	-2.1
$\omega_{1,0}^V$	28/3

Table 1: Experimental value of coupling to the vector current [18] (first row); couplings entering the vector meson DAs at the scale $\mu_0 = 1 \text{ GeV}$.

V	ϕ
$m_V f_{3V}^A [\text{GeV}^2]$	$3.37 \cdot 10^{-3}$
$m_V f_{3V}^V [\text{GeV}^2]$	$5.26 \cdot 10^{-3}$

Table 2: Decay constants obtained from Eq. (12).

2.5 Cross section and b-slope

The imaginary part of the amplitude in Eq. (1) which enters the expression of the cross section for transverse and longitudinal polarization, can be written as:

$$\sigma_L(\gamma^* p \rightarrow V p) = \frac{1}{16\pi B(Q^2)} \left| \frac{T_{00}(s, Q^2)}{W^2} \right|^2, \quad (29)$$

$$\sigma_T(\gamma^* p \rightarrow V p) = \frac{1}{16\pi B(Q^2)} \left| \frac{T_{11}(s, Q^2)}{W^2} \right|^2, \quad (30)$$

where $B(Q^2)$ is a slope parameter which depends on the virtuality of the photon and it is parametrized in the present analysis as follows [19]:

$$B(Q^2) = \beta_0 - \beta_1 \log \left[\frac{Q^2 + m_\phi^2}{m_{J/\psi}^2} \right] + \frac{\beta_2}{Q^2 + m_\phi^2}, \quad (31)$$

with $\beta_0 = 7.0 \text{ GeV}^{-2}$, $\beta_1 = 1.1 \text{ GeV}^{-2}$ and $\beta_2 = 1.1$.

The full cross section is a sum of longitudinal and transverse components, and it reads

$$\sigma_{tot}(\gamma^* p \rightarrow V p) = \sigma_T + \epsilon \sigma_L, \quad (32)$$

where $\epsilon \approx 1$ due to HERA kinematics.

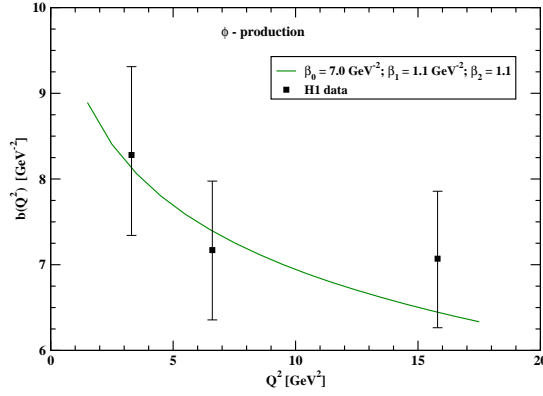


Figure 1: Q^2 -dependence of the b-slope for ϕ -meson production in the $\gamma^* p \rightarrow \phi p$ reaction. Due to the high uncertainty of the experimental data, we keep the standard choice of β_0 , β_1 and β_2 parameters from Ref. [19] for all our results.

3 Numerical Results

In what follows we present theoretical predictions adopting two different UGD models:

- the Ivanov-Nikolaev parametrization, endowed with soft and hard components to probe both large and small transverse momentum region (see Ref. [15] for further details);
- the model provided by Golec-Biernat and Wüsthoff (GBW), which derives from the dipole cross section for the scattering of a $q\bar{q}$ pair off a nucleon [20].

We start from calculating longitudinal cross section using the formalism described in the previous section. In Fig.2 we show results of our calculation for the Ivanov-Nikolaev (left panel) and GBW (right panel) UGDs. In order to get these predictions, the asymptotic DA has been used. This calculation has been obtained for $W = 75$ GeV. We observe that the cross sections obtained for massless strange quarks (black solid line) overestimate the experimental cross section below $Q^2 < 10$ GeV². This is very different for ρ^0 production to be discussed elsewhere. In both cases we present also our results when using quarks/antiquarks with effective masses (as described in the previous section). Then a good description of the experimental data is obtained for both the Ivanov-Nikolaev and GBW UGDs. How much the cross section depends on the quark mass is discussed in Fig.3 for asymptotic (left panel) and LCWF (right panel) DAs, respectively. The best description of the data is obtained with $m_q = 0.5$ GeV. A similar result was found in Ref. [3] within the k_T -factorization approach with a Gaussian $s\bar{s}$ light-cone wave function for the ϕ meson.

Now we pass to the transverse cross section as a function of photon virtuality.

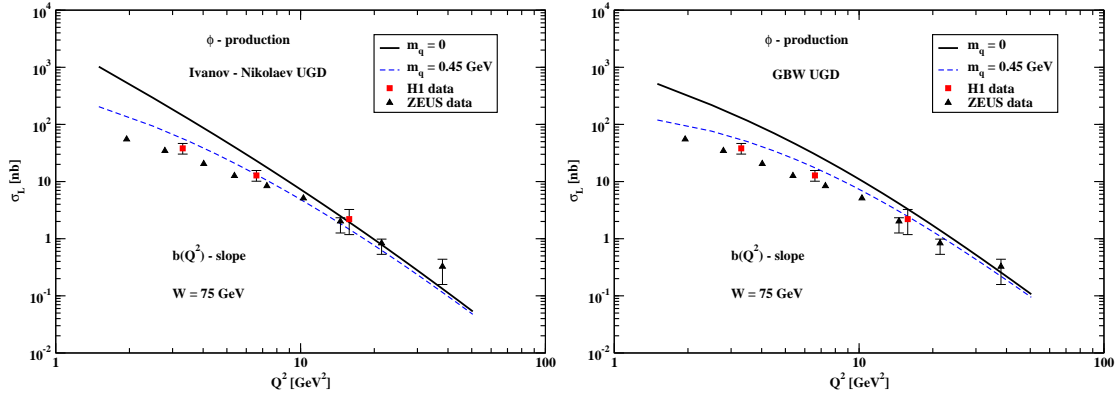


Figure 2: Q^2 -dependence of longitudinal cross section σ_L of ϕ -meson production, at $W = 75$ GeV, in comparison with experimental data of the H1 [13] and ZEUS [14] collaborations. The result is obtained within the k_T -factorization using the Ivanov-Nikolaev UGD model (left panel) and the GBW one (right panel). The solid lines are for the case when the strange-quark mass is neglected and the dashed lines for the strange-quark mass fixed at $m_q = 0.45$ GeV. In both cases, the asymptotic distribution amplitude (DA) is used.

In Fig.4 we show the cross section separately for the Wandzura-Wilczek and genuine three-parton contributions. In this calculation massless quarks were used. We observe that the transverse cross section for the genuine three-parton contribution is rather small. However, the WW contribution for massless quarks, similarly as for the longitudinal cross section, overpredicts the H1 and ZEUS data. Can this be explained as due to the mass effect discussed in the previous section?

In Fig.5 we show how the WW contribution changes when including the mass effect discussed in the previous section. Inclusion of the mass effect improves the description of the H1 and ZEUS experimental transverse cross section. The description is, however, not perfect. In Fig.5 we present a similar result for both UGD models. Unlike for the longitudinal cross section, here the GBW overpredicts the experimental data in the whole range of virtuality, while the Ivanov-Nikolaev model only at smaller Q^2 values. A reasonable result is obtained when including mass effect.

We wish to show also results for the σ_L/σ_T ratio (see Fig.6) as a function of photon virtuality Q^2 for the Ivanov-Nikolaev and GBW UGDs. In this calculation the quark mass was fixed for $m_q = 0.45$ GeV. The Ivanov-Nikolaev UGD much better describes the H1 and ZEUS data.

How much the ratio depends on the effective quark mass parameter? This is shown in Fig.7. The ratio is much less sensitive to the quark mass than the polarized cross sections σ_L and/or σ_T separately. So the extraction of the mass parameter from the normalized cross section is preferred.

Now we shall show the total cross section σ_{tot} as a function of virtuality. In Fig. 8 we show both longitudinal and transverse components as well as their sum.

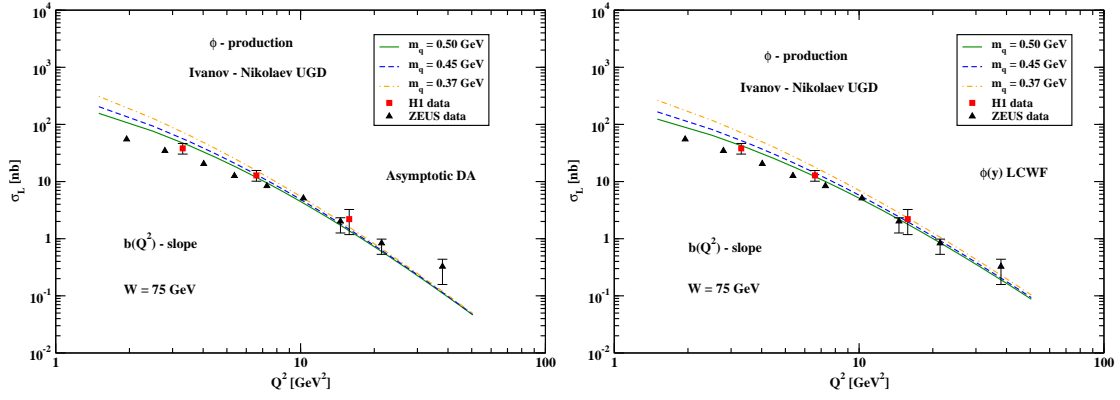


Figure 3: σ_L for the asymptotic DA (left panel) and for the LCWF DA (right panel). Results for three different strange-quark-mass values are shown. Predictions are given using the Ivanov-Nikolaev UGD model.

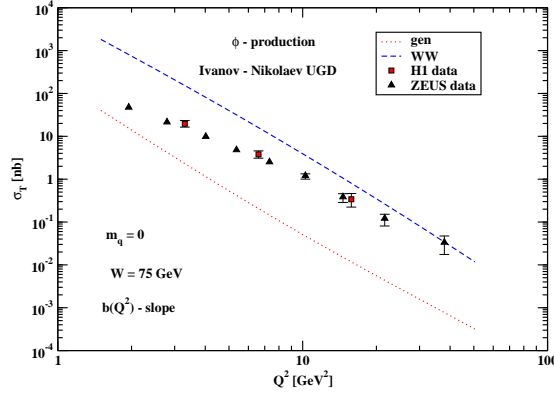


Figure 4: Q^2 -dependence of the transverse cross section σ_T neglecting the quark mass m_q . The WW and the genuine three-parton contributions are shown separately.

The transverse cross section is somewhat steeper (falls faster with virtuality) than the longitudinal one. The comparison with the HERA data is presented in Fig.9. The GBW UGD better describes the experimental data at small photon virtualities. There seems to be a small inconsistency of the H1 and ZEUS data at larger virtualities.

So far we did not consider skewedness effects and the real part of the $\gamma^* p \rightarrow \phi p$ amplitude. Both these corrections can be calculated from the energy dependence of the forward amplitude. Defining

$$\Delta_{\mathbf{IP}} = \frac{\partial \log \left(\Im m T_{\lambda_V \lambda_\gamma}(s, Q^2)/s \right)}{\partial \log(1/x)}, \quad (33)$$

we can calculate the real part from

$$\rho = \frac{\Re T_{\lambda_V \lambda_\gamma}(s, Q^2)}{\Im m T_{\lambda_V \lambda_\gamma}(s, Q^2)} = \tan \left(\frac{\pi \Delta_{\mathbf{IP}}}{2} \right). \quad (34)$$

The skewedness correction is obtained from multiplying the forward amplitude by

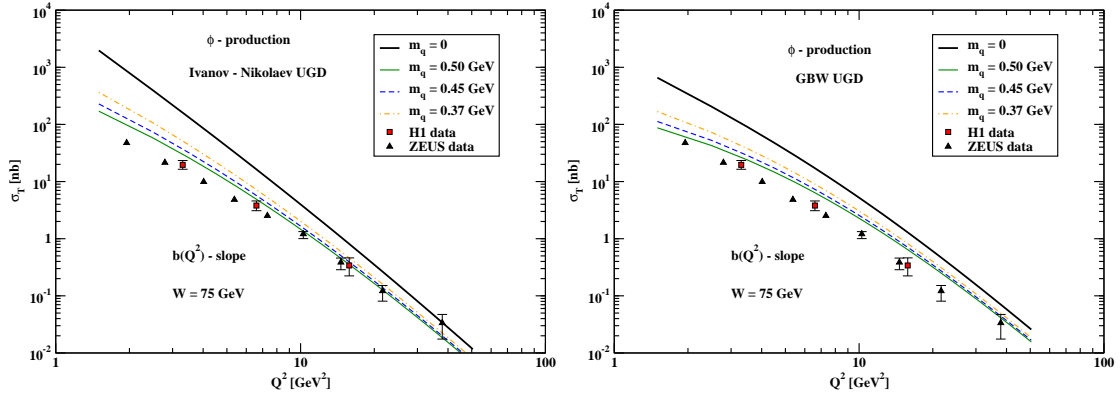


Figure 5: Q^2 -dependence of the transverse cross section σ_T for the ϕ -meson production in the $\gamma^* p \rightarrow \phi p$ reaction, at $W = 75$ GeV, in comparison with the H1 [13] and ZEUS [14] experimental data. The result is obtained within the k_T -factorization using the Ivanov-Nikolaev UGD model (left panel) and the GBW one (right panel). The thick solid line is for the case when the strange-quark mass is neglected. The thin lines show the result for the three different values of the strange-quark mass. In both cases, the curves were obtained with the asymptotic choice of the distribution amplitude (DA).

the factor [21]:

$$R_{\text{skewed}} = \frac{2^{2\Delta_{\mathbf{P}}+3}}{\sqrt{\pi}} \cdot \frac{\Gamma(\Delta_{\mathbf{P}} + 5/2)}{\Gamma(\Delta_{\mathbf{P}} + 4)}. \quad (35)$$

Now we wish to show our estimates of these corrections. We show results for longitudinal (Fig. 10) and transverse (Fig. 11) components separately. The effect is not too big but cannot be neglected. The effect of the skewedness is much larger than the effect of the inclusion of the real part. We observe that the effect of the skewedness does not cancel in the σ_L/σ_T ratio as can be seen in Fig. 12.

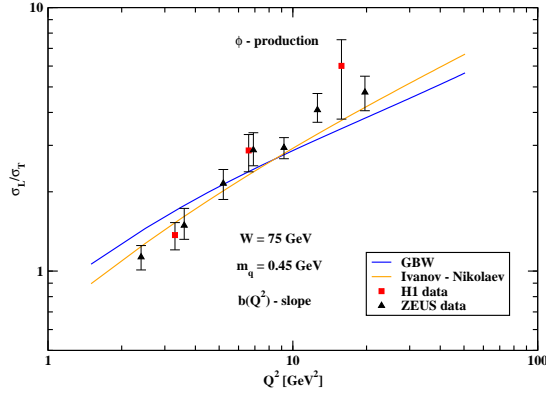


Figure 6: Q^2 -dependence of cross section ratio σ_L/σ_T for the ϕ -meson production in the $\gamma^* p \rightarrow \phi p$ reaction, at $W = 75$ GeV, in comparison with experimental data of the H1 [13] and ZEUS [14] collaboration. The prediction is performed in the k_T -factorization approach, using both UGD models: the Ivanov-Nikolaev and the GBW one. The strange-quark mass is fixed here at $m_q = 0.45$ GeV.

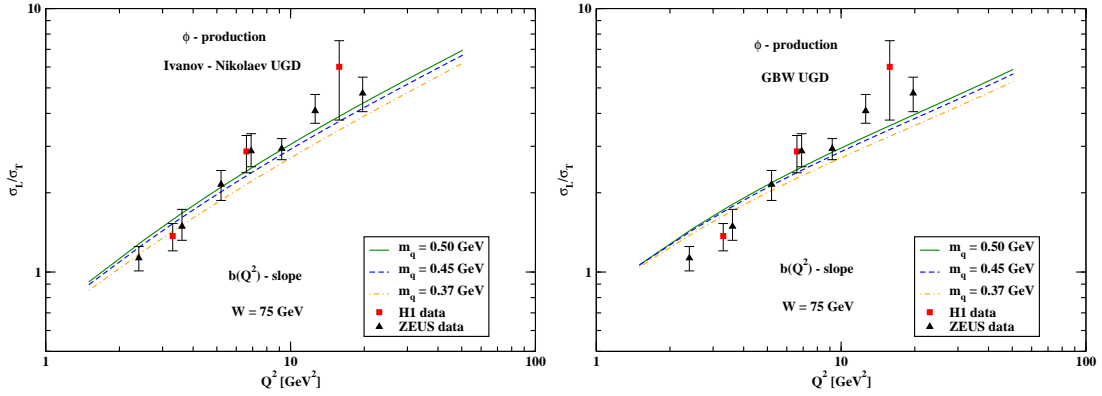


Figure 7: Q^2 -dependence of the cross section ratio σ_L/σ_T for three different quark-mass values m_q using the Ivanov-Nikolaev (left panel) and the GBW (right panel) UGDs.

4 Conclusions

In the present paper we have used a recently formulated hybrid formalism for the production of ϕ meson in the $\gamma^* p \rightarrow \phi p$ reaction using unintegrated gluon distributions and meson distribution amplitudes. In this formalism the $\gamma^* \rightarrow \phi$ impact factor is calculated in collinear-factorization using (collinear) distribution amplitudes. So far this formalism was used only for massless quarks/antiquarks (e.g. for ρ^0 meson production). Both twist-2 and twist-3 contributions are included. The impact factor for the $p \rightarrow p$ transition are expressed in terms of UGDs. Two different UGD models have been used.

We have shown that for massless quarks the genuine three-parton contribution is more than order of magnitude smaller than the WW one. Therefore in this paper we have concentrated on the WW component.

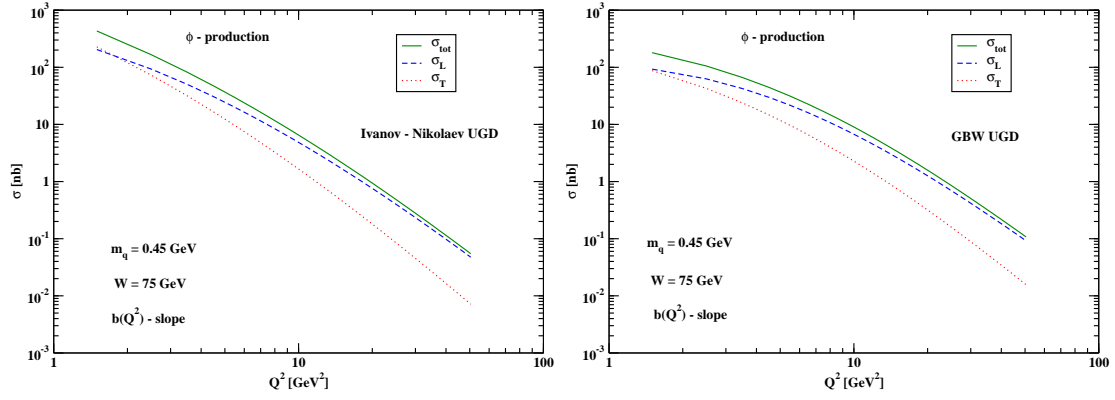


Figure 8: Longitudinal, transverse and total cross sections as functions of Q^2 using the Ivanov-Nikolaev (left panel) and the GBW (right panel) UGDs.

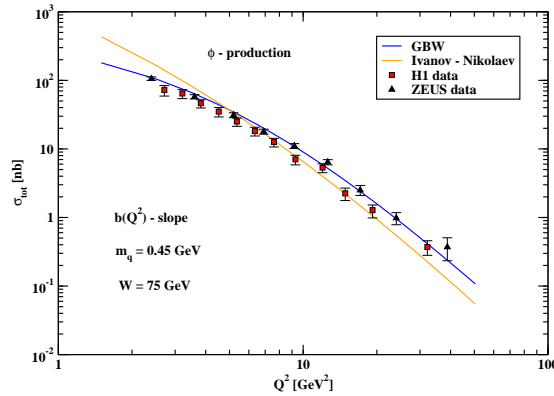


Figure 9: Q^2 dependence of total cross section σ_{tot} at $W = 75$ GeV for both UGD models in comparison with the H1 [13] and ZEUS [14] experimental data.

We have observed too quick rise of the cross section when going to smaller photon virtualities compared to the experimental data measured by the H1 and ZEUS collaborations at HERA. This was attributed to the massless quarks/antiquarks. We have proposed how to include effective quark masses into the formalism. Corresponding distribution amplitudes were calculated and have been used in the present approach. With effective quark mass $m_q \sim 0.5$ GeV a good description of the H1 and ZEUS data has been achieved for the Ivanov-Nikolaev and GBW UGDs down to $Q^2 \sim 4$ GeV². This value of the strange quark mass is similar as the one found in Ref. [3], where the k_T -factorization formalism with $s\bar{s}$ light-cone wave function of the ϕ meson was used for real photoproduction.

We have estimated also the skewedness effect which turned out to be not too big but not negligible. We have shown some residual effect of the skewedness for the ratio of longitudinal-to-transverse cross sections.

Acknowledgment A.D. Bolognino thanks University of Cosenza and INFN for support of her stay in Kraków. We are indebted to Alessandro Papa for a discus-

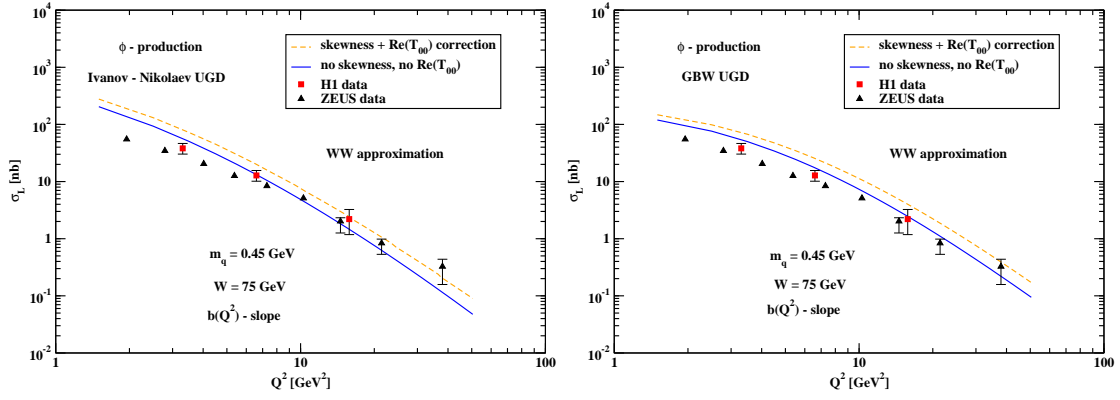


Figure 10: An estimation of the skewedness effects and the real part of the amplitude for the longitudinal cross section σ_L calculated in the WW approximation using the Ivanov-Nikolaev (left panel) and GBW (right panel) UGDs.

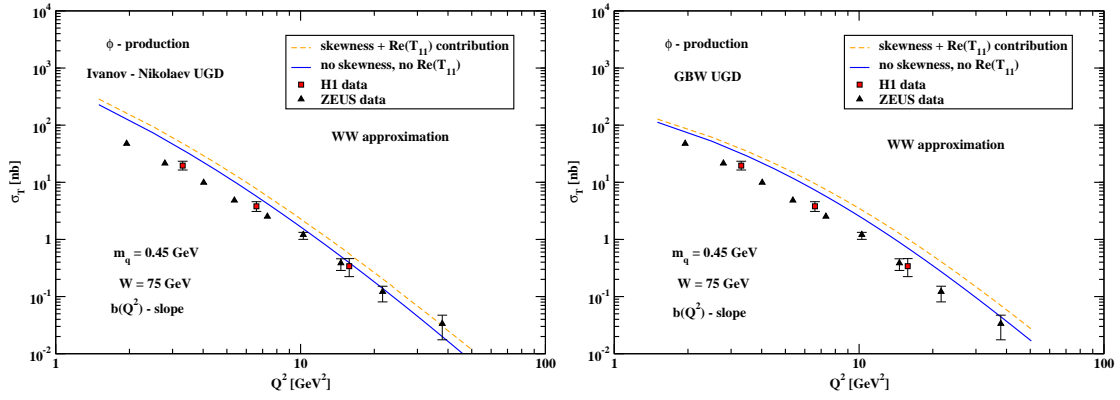


Figure 11: An estimation of the skewedness effects and the real part of the amplitude for the transverse cross section σ_T calculated in the WW approximation using the Ivanov-Nikolaev (left panel) and GBW (right panel) UGDs.

sion.

This study was partially supported by the Polish National Science Center grant UMO-2018/31/B/ST2/03537 and by the Center for Innovation and Transfer of Natural Sciences and Engineering Knowledge in Rzeszów.

References

- [1] I.P. Ivanov, N. N. Nikolaev and A. A. Savin, Phys. Part. Nucl. **37**, 1 (2006) [hep-ph/0501034].
- [2] A. Accardi *et al.*, Eur. Phys. J. A **52**, no. 9, 268 (2016) [arXiv:1212.1701 [nucl-ex]].
- [3] A. Cisek, W. Schäfer and A. Szczurek, Phys. Lett. B **690** (2010) 168 [arXiv:1004.0070 [hep-ph]].

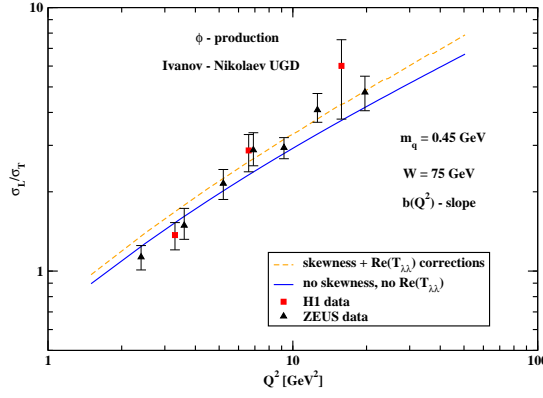


Figure 12: An estimation of the skewedness effects and the real part of the amplitude are shown for the cross sections ratio σ_L/σ_T through the Ivanov-Nikolaev UGD.

- [4] I.V. Anikin, D.Yu. Ivanov, B. Pire, L. Szymanowski and S. Wallon, Nucl. Phys. B **828**, 1 (2010) [arXiv:0909.4090 [hep-ph]].
- [5] I.V. Anikin, A. Besse, D.Yu. Ivanov, B. Pire, L. Szymanowski and S. Wallon, Phys. Rev. D **84** (2011) 054004 [arXiv:1105.1761 [hep-ph]].
- [6] A.D. Bolognino, F.G. Celiberto, D.Yu. Ivanov, A. Papa, Eur. Phys. J. C **78** (2018) 1023.
- [7] A.V. Radyushkin, JINR-P2-10717 (Dubna, 1977), [hep-ph/0410276]; A.V. Efremov and A.V. Radyushkin, Theor. Math. Phys. **42**, 97 (1980) [Teor. Mat. Fiz. **42**, 147 (1980)]; Phys. Lett. **94B**, 245 (1980).
- [8] G.P. Lepage and S.J. Brodsky, Phys. Lett. **87B**, 359 (1979).
- [9] G.P. Lepage and S.J. Brodsky, Phys. Rev. D **22**, 2157 (1980).
- [10] V.L. Chernyak and A.R. Zhitnitsky, Phys. Rept. **112**, 173 (1984).
- [11] P. Ball, V.M. Braun, Y. Koike and K. Tanaka, Nucl. Phys. B **529** (1998) 323 [hep-ph/9802299].
- [12] C. Adloff *et al.* [H1 Collaboration], Phys. Lett. B **483**, 360 (2000) [hep-ex/0005010].
- [13] F.D. Aaron *et al.* [H1 Collaboration], JHEP **1005**, 032 (2010) [arXiv:0910.5831 [hep-ex]].
- [14] S. Chekanov *et al.* [ZEUS collaboration], Nucl. Phys. B **718** (2005) [arXiv:0504.010v1 [hep-ph]].
- [15] I.P. Ivanov, N.N. Nikolaev, Phys. Rev. D **65** (2002) 054004 [hep-ph/0004206].

- [16] D.Yu. Ivanov, M.I. Kotsky and A. Papa, Eur. Phys. J. C **38**, 195 (2004) [hep-ph/0405297].
- [17] D.Yu. Ivanov and A. Papa, Nucl. Phys. B **732**, 183 (2006) [hep-ph/0508162].
- [18] M. Tanabashi et al. [Particle Data Group], Phys. Rev. D **98**, no. 3, 030001 (2018).
- [19] J. Nemchik, N.N. Nikolaev, E. Predazzi, B.G. Zakharov and V. R. Zoller, J. Exp. Theor. Phys. **86** (1998) 1054 [Zh. Eksp. Teor. Fiz. **113** (1998) 1930] doi:10.1134/1.558573 [hep-ph/9712469].
- [20] K.J. Golec-Biernat and M. Wusthoff, Phys. Rev. D **59**, 014017 (1998) [arXiv:hep-ph/9807513 [hep-ph]].
- [21] A.G. Shuvaev, K.J. Golec-Biernat, A.D. Martin and M.G. Ryskin, Phys. Rev. D **60**, 014015 (1999) [hep-ph/9902410].